



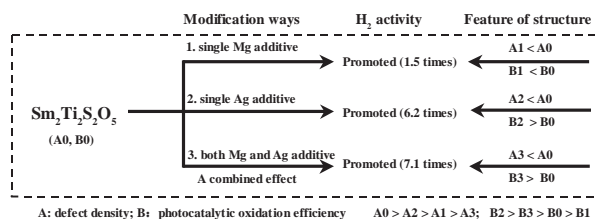
## Contents

### REGULAR ARTICLES

#### Improvement of the photocatalytic hydrogen evolution activity of $\text{Sm}_2\text{Ti}_2\text{S}_2\text{O}_5$ under visible light by metal ion additives

pp 1–7

Fuxiang Zhang, Kazuhiko Maeda, Tsuyoshi Takata, Kazunari Domen\*

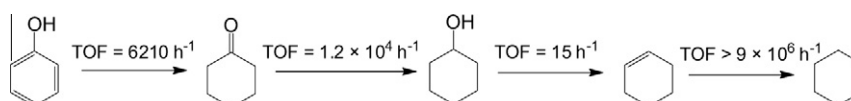


Metal ion modification of oxysulfide ( $\text{Sm}_2\text{Ti}_2\text{S}_2\text{O}_5$ ) could efficiently promote photocatalytic  $\text{H}_2$  evolution from  $\text{Na}_2\text{S}$ – $\text{Na}_2\text{SO}_3$  solution under visible light, and a further promotion originating from combined effect of Mg and Ag was demonstrated.

#### Aqueous-phase hydrodeoxygenation of bio-derived phenols to cycloalkanes

pp 8–16

Chen Zhao, Jiayue He, Angeliki A. Lemonidou, Xuebing Li, Johannes A. Lercher\*

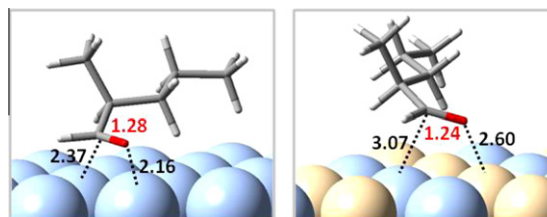


Hydrodeoxygenation of phenol and substituted phenols over dual-functional Pd/C and  $\text{H}_3\text{PO}_4$  catalysts proceeds via stepwise hydrogenation of the aromatic ring, transformation of the cyclic enol to the corresponding ketone, hydrogenation of the cycloalkanone to the cycloalkanol and its subsequent dehydration as well as the hydrogenation of the formed cycloalkene.

#### Conversion of furfural and 2-methylpentanal on Pd/SiO<sub>2</sub> and Pd–Cu/SiO<sub>2</sub> catalysts

pp 17–27

Surapas Sitthisa, Trung Pham, Teerawit Prasomsri, Tawan Sooknoi, Richard G. Mallinson, Daniel E. Resasco\*

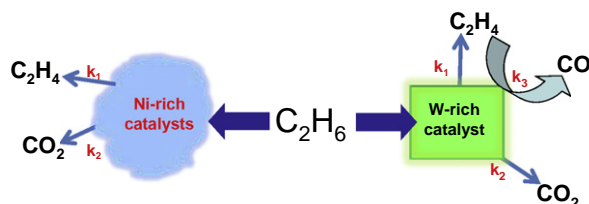


Methylpentanal on monometallic Pd and bimetallic Pd–Cu clusters adsorbed in an  $\eta^2$  configuration. This species is the precursor for the acyl species that results in decarbonylation. The presence of Cu greatly reduces the Pd–metal bond strength and the rate of aldehyde decarbonylation.

**Oxidative dehydrogenation of ethane over Ni–W–O mixed metal oxide catalysts**

pp 28–39

B. Solsona, J.M. López Nieto\*, P. Concepción, A. Dejoz, F. Ivars, M.I. Vázquez

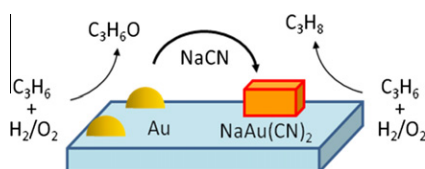


Ni–W–O mixed oxides have been tested in the oxidative dehydrogenation of ethane: ethane conversion influences ethylene selectivity in W-rich catalysts, while it hardly influences ethylene selectivity in Ni-rich catalysts.

**Effect of gold oxidation state on the epoxidation and hydrogenation of propylene on Au/TS-1**

pp 40–49

Jason Gaudet, Kyoko K. Bando, Zhaoxia Song, Tadahiro Fujitani, Wei Zhang, Dang Sheng Su, S. Ted Oyama\*

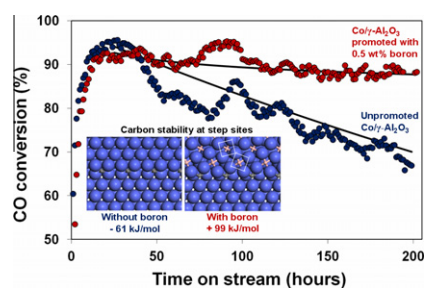


Treatment of gold samples supported on TS-1 with sodium cyanide solutions resulted in the precipitation of gold (I) cyanide. When this occurred, the selectivity of the reaction of propylene with hydrogen and oxygen mixtures shifted from propylene oxide to propylene, a selectivity characteristic of Pt.

**Effect of boron promotion on the stability of cobalt Fischer–Tropsch catalysts**

pp 50–59

Kong Fei Tan, Jie Chang, Armando Borgna\*, Mark Saeys\*

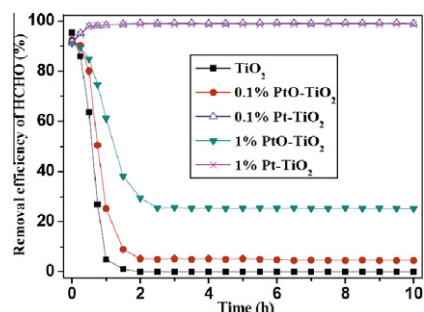


Boron promotion enhances the stability of Co/γ-Al<sub>2</sub>O<sub>3</sub> catalysts during Fischer–Tropsch synthesis. Density functional theory shows that boron is stable near step sites and reduces carbon stability by 160 kJ/mol.

**Complete elimination of indoor formaldehyde over supported Pt catalysts with extremely low Pt content at ambient temperature**

pp 60–67

Haibao Huang\*, Dennis Y.C. Leung\*

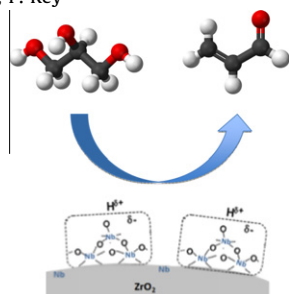


Nearly 100% HCHO conversion was obtained over the reduced Pt/TiO<sub>2</sub> catalysts even with 0.1% Pt loading. Metallic Pt rather than cationic Pt nanoparticles are the active centers for HCHO oxidation.

**New efficient and long-life catalyst for gas-phase glycerol dehydration to acrolein**

pp 68–76

P. Lauriol-Garbay, J.M.M. Millet\*, S. Loridant, V. Bellière-Baca, P. Rey

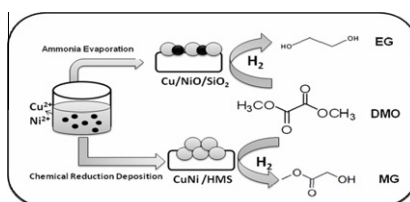


Zirconium and niobium mixed oxides have been shown to be selective catalysts for dehydration of glycerol to acrolein, at 300 °C in gas phase. The catalysts exhibit a selectivity to acrolein of approximately 72%, at nearly total glycerol conversion. The new catalysts distinguish themselves by their unique stability on stream that make them promising for industrial application.

**Influence of Ni species on the structural evolution of Cu/SiO<sub>2</sub> catalyst for the chemoselective hydrogenation of dimethyl oxalate**

pp 77–88

Anyuan Yin, Chao Wen, Xiaoyang Guo, Wei-Lin Dai\*, Kangnian Fan

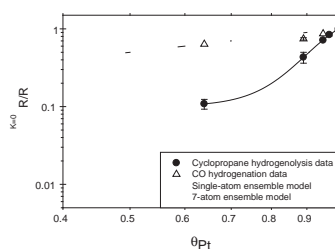


Cu–Ni/HMS catalyst exhibited excellent catalytic performance in chemoselective hydrogenation of dimethyl oxalate. Methyl glycolate (MG) and ethylene glycol (EG) could be effectively obtained via tuning the surface chemical states of nickel species.

**Structure sensitivity of cyclopropane hydrogenolysis on carbon-supported platinum**

pp 89–95

Jack Z. Zhang, Yu-Tung Tsai, Khunya Leng Sangkaewwattana, James G. Goodwin\* Jr.

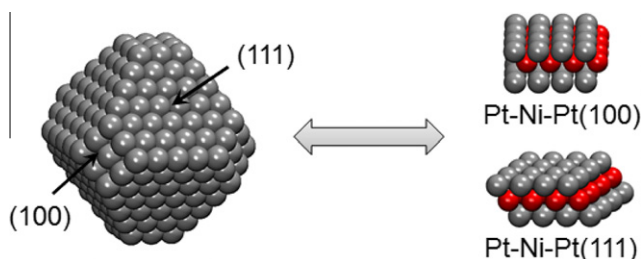


Although poisoning/blocking of Pt by K<sup>+</sup> appears to be non-uniform, reaction analysis strongly indicates the structure sensitivity of cyclopropane hydrogenolysis on Pt. Based on Martin’s model, the ensemble size required for this hydrogenolysis reaction appears to be ca. 7, whereas the structure insensitive CO hydrogenation reaction requires an ensemble size of ca. 1.

**Bridging the materials gap between single crystal and supported catalysts using polycrystalline Ni/Pt bimetallic surfaces for cyclohexene hydrogenation**

pp 96–103

Michael P. Humbert, Alan L. Stottlemeyer, Carl A. Menning, Jingguang G. Chen\*

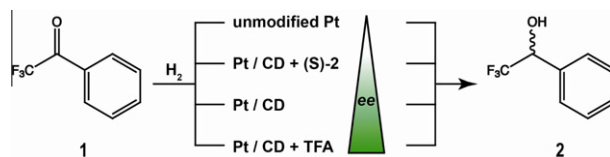


Experimental and theoretical studies are performed for the hydrogenation of cyclohexene on polycrystalline Ni/Pt bimetallic surfaces to bridge the materials gap between single crystal and more complex surfaces.

**Multiple cycle reaction mechanism in the enantioselective hydrogenation of  $\alpha,\alpha,\alpha$ -trifluoromethyl ketones**

pp 104–115

Z. Cakl, S. Reimann, E. Schmidt, A. Moreno, T. Mallat, A. Baiker\*

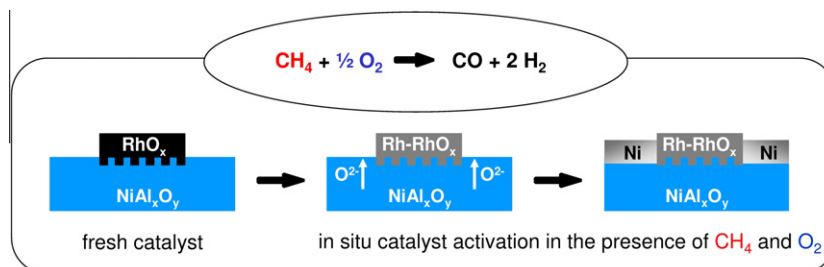


A combined catalytic and NMR study has uncovered a multiple cycle mechanism in the enantioselective hydrogenation of 2,2,2-trifluoroacetophenone (1) on cinchona-modified Pt. A key element is the involvement of the minor product (S)-1-phenyl-2,2,2-trifluoroethanol (2) in the enantioselection.

**Mechanistic origins of the promoting effect of tiny amounts of Rh on the performance of  $\text{NiO}_x/\text{Al}_2\text{O}_3$  in partial oxidation of methane**

pp 116–124

Claudia Berger-Karin, Jörg Radnik, Evgenii V. Kondratenko\*

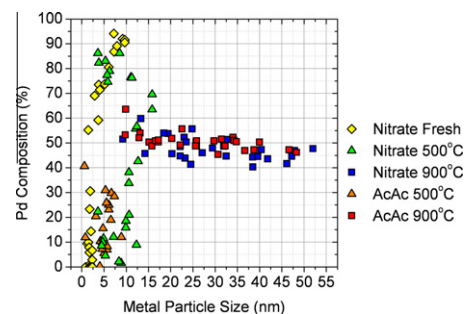


Mechanistic scheme of the synergetic effect of Rh on  $\text{NiO}_x(3 \text{ wt.}\%)/\text{Al}_2\text{O}_3$  in the POM reaction.

**Characterization of alumina-supported Pt and Pt–Pd NO oxidation catalysts with advanced electron microscopy**

pp 125–136

O.K. Ezekoye, A.R. Drews, H.-W. Jen, R.J. Kudla, R.W. McCabe, M. Sharma, J.Y. Howe, L.F. Allard, G.W. Graham\*, X.Q. Pan

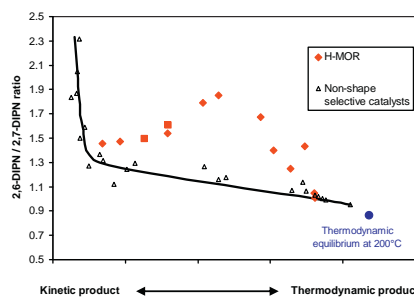


High angle annular dark field imaging along with energy dispersive spectroscopy were used to study the evolution of metal particle size and composition in alumina-supported Pt-Pd NO oxidation catalysts made using two precursors, acetylacetonate (AcAc) and nitrate, aged under oxidizing conditions. In spite of distinctly different initial metal distributions, aging led to very similar characteristics for both precursors.

**LETTERS TO THE EDITOR****Polemic against conclusions drawn in “Shape-selective diisopropylation of naphthalene in H-Mordenite: Myth or reality?” (J. Catal., 270 (2010) 60–66)**

pp 137–141

Robert Brzozowski



Some experimental results obtained in alkylation of naphthalene to diisopropylnaphthalene over H-MOR cannot be explained by kinetics, thermodynamics and analytical errors, as suggested in the article mentioned in the title; therefore, shape-selective diisopropylation of naphthalene over H-mordenite is still the reality.

---

**Reply to the letter of Robert Brzozowski concerning the conclusions drawn in “Shape-selective diisopropylation of naphthalene in H-Mordenite: Myth or reality?”** pp 142–143

Wim Buijs, Pierre A. Jacobs, Johan A. Martens\*

---